

# Proposed Low-Power High-Speed Microring Resonator-Based Switching Technique for Dynamically Reconfigurable Optical Interconnects

Chander Kochar, *Student Member, IEEE*, Avinash Kodi, *Student Member, IEEE*, and Ahmed Louri, *Senior Member, IEEE*

**Abstract**—The dynamic bandwidth re-allocation (DBR) technique balances traffic by re-allocating bandwidth from under-utilized links to over-utilized links in a network. In this letter, we propose a nonblocking, fast, low-power, and integratable optical switch that enables DBR. The basic building blocks of the proposed switch are silicon-on-insulator-based microring resonators. Analytical and numerical studies show that the active switch design gives similar performance in throughput and latency, while reducing cost (number of lasers) and area significantly when compared to implementation of DBR with only passive components. There is a slight increase in power ( $\sim 0.4\%$  for worst-case traffic pattern) using the active switch implementation.

**Index Terms**—Dynamic bandwidth re-allocation (DBR), microring resonators, reconfigurable architectures.

## I. INTRODUCTION

THE availability of small low-power integratable optical switches are key to the realization of dense photonic integrated circuits (PICs). A considerable amount of work is available in the literature on optical switches; however, the microelectromechanical-systems-based switches have  $\sim 1$  ms or higher response time, the fast electrooptic LiNbO<sub>3</sub>-based switches require a minimum actuation voltage of 5 V and the III–V semiconductor heterostructure-based switches are difficult to integrate on a chip [1]. The active row–column switch design proposed in this letter enables any-to-any routing (i.e., any wavelength can be routed to any destination), while overcoming the above mentioned problems. The number of transmitters required for the active row–column switch scales as  $O(n)$  and does not use arrayed waveguide gratings (AWGs), which are generally bulky and difficult to integrate. Silicon-on-insulator (SOI)-based microring resonators are used as the basic building blocks. These microring resonators can be used to build  $1 \times 2$  wavelength-selective optical switches that are fast ( $\sim 10$  ns), small ( $\sim 10$   $\mu\text{m}$  diameter), power efficient ( $\sim 19$   $\mu\text{W}$ ), and can be fabricated using standard complementary metal–oxide semiconductor (CMOS) technology [2], [3]. Two distinct advantages of using SOI-based microring resonators are: 1) They can be fabricated using existing CMOS

technology, allowing for a low-cost solution to dense PICs, and 2) they allow high confinement of light enabling micrometer scale devices, which results in low area and power overheads.

One important application of optical interconnects is implementation of dynamic bandwidth re-allocation (DBR). Application of DBR techniques allows for a more even distribution of load among the different links and channels thereby improving throughput and latency. DBR has previously been implemented in [4] using only passive optical components such as couplers and AWGs. This approach has two main drawbacks: 1) It requires  $O(n^2)$  lasers where  $n$  is the number of transmitters per board, which results in high cost, and 2) it made use of AWGs which are generally bulky and can cause integration problems.

## II. DBR IMPLEMENTATION

E-RAPID is an optoelectronic architecture designed to cater to the large bandwidth and low latency of high-performance computing systems. Due to space limitations and reviewer comments, we refer the reader to [4] for more details about the architecture.

### A. DBR With Active Components

A brief explanation of a  $1 \times 2$  microring resonator switch is given before describing the details of the proposed row–column switch. Consider a ring resonator with one input port ( $I_0$ ) and two output ports ( $O_0$  and  $O_1$ ) with  $I_0$  and  $O_0$  on opposite ends of the same waveguide. On applying a voltage across the ring resonator, light will travel from  $I_0$  to  $O_0$ , and if no voltage is applied, light flows from  $I_0$  to  $O_1$  [3].

The proposed switch consists of two-dimensional row–column switches as shown in Fig. 1. In contrast to the passive case, the number of lasers required is now  $n$ . The default or static output for transmitter  $k$  remains the same as described by the routing and wavelength assignment [4]. In order to route transmitter  $k$  to some other output, we make use of the column switches. The row and column switches are themselves  $2 \times 2$  switches. Due to the wavelength-selective nature of the rings, light at each input can be individually routed to any output. For an  $n \times n$  switch matrix, we need  $n$  row switches and  $n$  column switches.

The detailed implementation of the proposed row–column switch is shown in Fig. 2(a). A row switch requires only one ring resonator, which is resonant with the light from the corresponding transmitter ( $I_{R1}$ ). Input from the previous column switch ( $I_{R0}$ ) exits the matrix by default at ( $O_{R0}$ ). The two exit points of the row switch,  $O_{R0}$  results in an outlet to leave the switch matrix, whereas  $O_{R1}$  sends the signal to the corresponding column switch. Of the two inputs to the column

Manuscript received April 23, 2007; revised June 1, 2007. This work was supported by National Science Foundation (NSF) Grant CCR-0309537 and Grant CCF-0538945.

The authors are with the Department of Electrical and Computer Engineering, The University of Arizona, Tucson, AZ 85721 USA (e-mail: louri@ece.arizona.edu).

Color versions of one or more of the figures in this letter are available online at <http://ieeexplore.ieee.org>.

Digital Object Identifier 10.1109/LPT.2007.902347

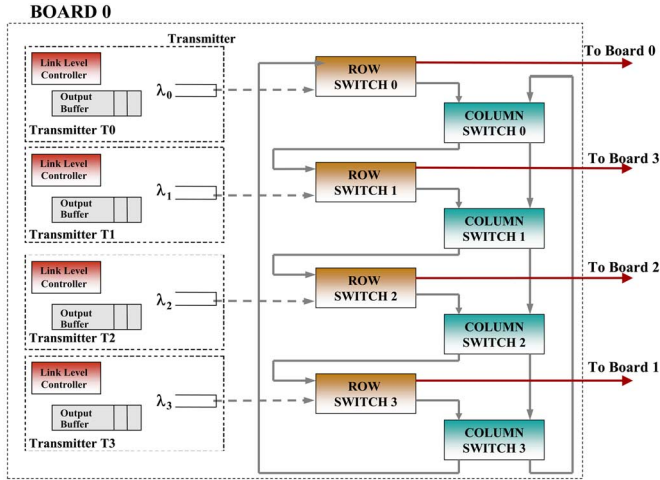


Fig. 1. Implementation of DBR with an active switch.

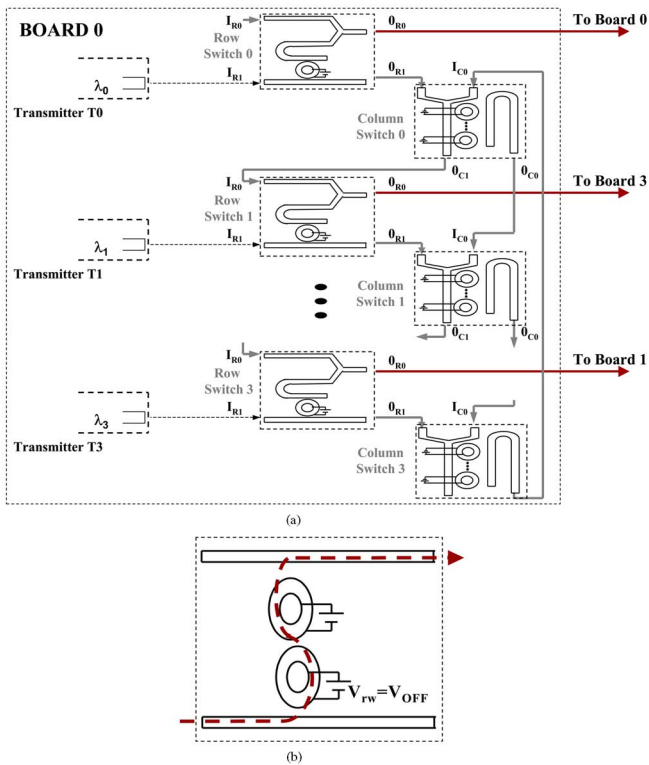


Fig. 2. (a) Detailed implementation of row-column switch.  $I_{R0}(= O_{C1})$  is the input from previous column switch,  $I_{R1}$  is input from transmitter,  $O_{R0}$  is the exit point from the switch matrix,  $O_{R1}$  is input to next column switch, and  $O_{C0}$  leads to the next column switch. (b) Implementation of row switch using two rings.  $V_{rw}$  is the corresponding control voltage of wavelength  $w$ .

switch,  $I_{C1}$  is the same as  $O_{R1}$ , while  $I_{C0}$  is the input from the previous column switch. There are  $n$  rings in the column switch which enable any input signal to be routed to any one of the two outputs independent of the other signals. Of the two output signals  $O_{C1}$  connects to  $I_{R0}$  of the next row switch where as  $O_{C0}$  connects to  $I_{C0}$  of the next column switch. By suitably controlling the applied voltages,  $V_{rw}$  (row voltage corresponding to wavelength  $w$ ), and  $V_{C0}, V_{C1}, \dots, V_{Cw}, V_{Cw+1}, \dots, V_{CN-1}$  (column voltages corresponding to the entire wavelength set,

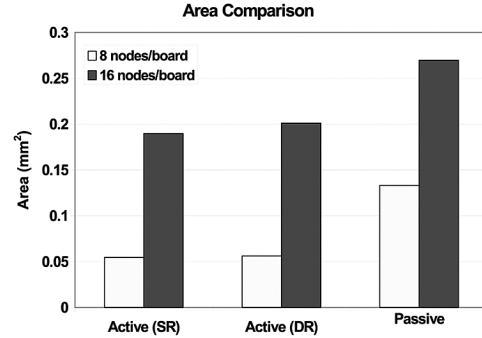


Fig. 3. Area comparison for switch matrix using different design methodologies. SR—single ring; DR—double ring.

$\Lambda = \lambda_0, \lambda_1, \dots, \lambda_{N-1}$ ) to either  $V_{ON}$  or  $V_{OFF}$ , we can perform any-to-any switching (one-to-one, many-to-one, all-to-one) of all the wavelengths.

Another design consideration would be to use two rings per wavelength instead of one. Although this would increase area and power loss, it has certain advantages: 1) Both the coupler and the u-bend can be removed for the row switch [as shown in Fig. 2(b)]. 2) The u-bend from the column switch is no longer required. 3) Higher order filters provide better filtering characteristics with decreased adjacent channel crosstalk [5]. Also, since only the lower ring requires to be turned ON or OFF, there will be no extra penalty in terms of electrical power consumption if two rings are used instead of one.

## B. Area and Cost Analysis

The area overhead of the microring resonator is calculated from [6], where the effective radius of a microring resonator was calculated to be  $10.5 \mu\text{m}$ . For the u-bend, the inner radius was assumed to be  $3 \mu\text{m}$  to negate the effect of bending losses and the coupler fits into an area of  $25 \mu\text{m}^2$  [7]. On using two rings per switch instead of one, the total length was estimated to be  $31.5 \mu\text{m}$ . Based upon the above values for an  $n \times n$  switch matrix, the total area of 1 row switch + 1 column switch was calculated to be  $(1770 + 630n) \mu\text{m}^2$  when using a single ring and  $(1471.5 + 693n) \mu\text{m}^2$  when using a double ring. From [8], the area of a  $4 \times 4$  SOI-based AWG is  $425 \times 155 \mu\text{m}^2$ . Since there is no data available on higher radix SOI-based AWGs, it was assumed that the area occupied by an AWG increases linearly with the radix (this is a reasonable assumption as it results in each dimension increasing by a factor of 1.4). The comparison of the area occupied by each method is shown in Fig. 3 (it should be noted that on-chip electrical wiring is not included in the area analysis). When comparing the filtering performance of AWGs and ring resonators, it was observed that the AWG has a  $-12$ -dB crosstalk [8], where as the crosstalk for a single ring resonator was negligible for  $1.3$ -nm spacing [2]. Reference [9] reports a second-order ring resonator-based filter with  $-30$ -dB crosstalk for  $150$ -GHz spacing. Cost analysis show that even for moderate values of  $n$ , the savings in terms of transmitters is significant when the active implementation is compared to the passive implementation. For example, in a  $64$  node E-RAPID system, while a passive switch would require  $64$  lasers per board, the active switch requires only  $8$ , thus saving on  $56$  lasers per board or  $448$  lasers for the entire system.

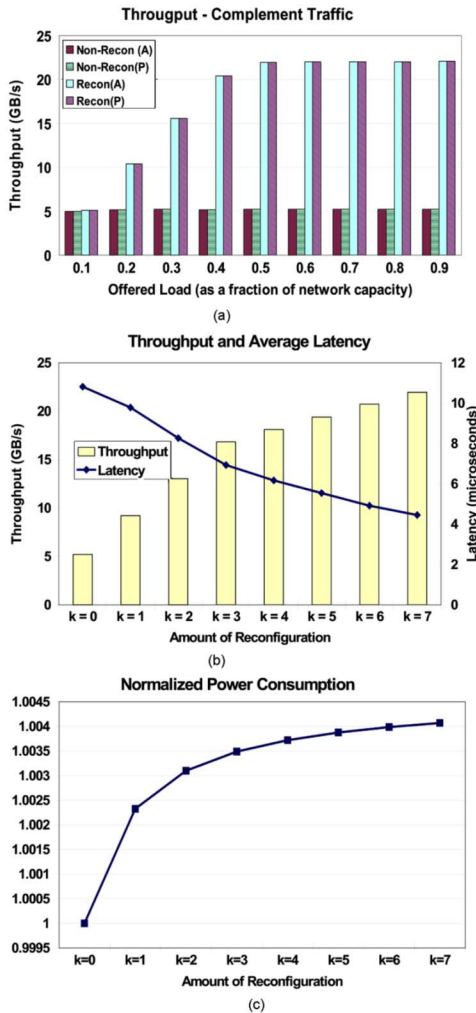


Fig. 4. Performance results for a 64-node E-RAPID system (a) throughput (b) throughput and latency variation with frequency of reconfiguration, (c) normalized power consumption.

### III. PERFORMANCE EVALUATION

E-RAPID is evaluated using NETSIM and YACSIM and cycle accurate simulations. Uniform traffic and several permutation patterns such as complement and butterfly were used to evaluate the performance of the active switch design. Due to space constraints, only a few of the results are discussed in this section. The electrical router was modeled to operate at a speed of 400 Mhz, with a bidirectional bandwidth of 12.8 Gb/s. Each reconfiguration window is 2000 cycles long and it take approximately 5 cycles to turn on a ring.

#### A. Results

Fig. 4(a) shows the effect of bandwidth re-allocation for complement traffic. Due to the nature of complement traffic, all the nodes on a board communicate with the same destination board. As a result, without bandwidth re-allocation, only one transmitter is active per board resulting in high latency and low throughput. A 400% increase in throughput is observed with reconfiguration enabled. Both active and passive switch devices show similar performance with and without reconfiguration. In fact, complement ensures maximum possible reconfiguration in the system and thus shows the worst-case power consumption

for the active switch design. Fig. 4(b) shows how throughput and latency vary as we change the amount of reconfiguration in a 64-node E-RAPID system with complement traffic and a load of 0.5. In the figure,  $k = i$  means  $i$  extra transmitters have been turned ON, i.e., the load can now be evenly distributed between  $i + 1$  different transmitters. As the amount of reconfiguration is increased, throughput increases and latency decreases. The decrease in latency is due to lower queuing and blocking delays observed by a packet. Fig. 4(c) shows how much extra power is consumed by the active switch design when compared to the passive switch design as the amount of reconfiguration is increased. Total power was calculated using the formula  $P_T = \sum_{j=0}^B N_{Bj} \times P_{Tx/Rx} + \sum_{j=0}^n N_{Rj} \times P_{ring}$ , where  $P_T$  is the total power consumed,  $B$  is total number of boards,  $N_{Bj}$  is the total number of packets transmitted by board  $j$ ,  $P_{Tx/Rx} = 43$  mW [4] is the power to transmit and receive a single 64-byte packet,  $N_{Rj}$  is the number of times a switch in the ON state is traversed by packets from board  $j$ , and  $P_{ring} = 100$   $\mu$ W [3] is the power consumed when a ring resonator is ON. In the worst case, the active switch consumes 0.41% more power when all the switches have been turned ON.

### IV. CONCLUSION

In this letter, a compact, integratable, and nonblocking optical switch matrix for implementing DBR is proposed. SOI-based microring resonators used as  $1 \times 2$  optical switches were the basic building blocks of the proposed active row-column switch. Analytical and simulation studies show that the proposed active implementation provides throughput and latency similar to the passive implementation while dramatically improving cost. There is a slight increase in power consumption (0.4% at most for the worst-case traffic) using the active switch matrix.

### REFERENCES

- [1] R. A. Soref and B. E. Little, "Proposed n-wavelength m-fiber wdm crossconnect switch using active microring resonators," *IEEE Photon. Technol. Lett.*, vol. 10, no. 8, pp. 1121–1123, Aug. 1998.
- [2] Q. Xu, B. Schmidt, S. Pradhan, and M. Lipson, "Micrometre-scale silicon electro-optic modulator," *Nature Lett.*, vol. 435, pp. 325–327, May 2005.
- [3] B. A. Small, B. G. Lee, K. Bergman, Q. Xu, and M. Lipson, "Multiple-wavelength integrated photonic networks based on microring resonator devices," *J. Opt. Netw.*, vol. 6, no. 2, pp. 112–120, Feb. 2007.
- [4] A. K. Kodi and A. Louri, "Power-aware bandwidth-reconfigurable optical interconnects for high-performance computing (hpc) systems," in *21st IEEE Int. Parallel and Distributed Processing Symp. (IPDPS'07)*, Long Beach, CA, Mar. 2007.
- [5] B. E. Little, S. T. Chu, H. A. Haus, J. Foresi, and J. P. Laine, "Microring resonator channel dropping filters," *J. Lightw. Technol.*, vol. 15, no. 6, pp. 998–1005, Jun. 1997.
- [6] L. Zhou and A. W. Poon, "Silicon electro-optic modulators using p-i-n diodes embedded 10-micron diameter microdisk resonators," *Opt. Express*, vol. 14, no. 15, pp. 6851–6857, Jul. 2006.
- [7] I. O'Connor, "Optical solutions for system level interconnects," in *Proc. 2004 Int. Workshop System Level Interconnect Prediction (SLIP'04)*, Paris, France, Feb. 2004, pp. 290–294.
- [8] P. Dumon, W. Bogaerts, D. V. Thourhout, D. Taillaert, and R. Baets, "Compact wavelength router based on a silicon-on-insulator arrayed waveguide grating pigtailed to a fiber array," *Opt. Express*, vol. 14, no. 2, pp. 664–669, Jan. 2006.
- [9] T. Barwicz, H. Byun, F. Gan, C. W. Holzwarth, M. A. Popovic, P. T. Rakich, M. R. Watts, E. P. Ippen, F. X. Kartner, H. I. Smith, J. S. Orcutt, R. J. Ram, V. Stojanovic, O. O. Olubuyide, J. L. Hoyt, S. Spector, M. Geis, M. Grein, T. Lyszczarz, and J. U. Yoon, "Silicon photonics for compact, energy-efficient interconnects[Invited]," *J. Opt. Netw.*, vol. 6, no. 1, pp. 63–73, Jan. 2007.